

# Vibrational Analysis of the Inelastic Neutron Scattering Spectrum of Tetramethylammonium Borohydride by Molecular Dynamics Simulations and Electronic Structure Calculations

Juergen Eckert,\* Thomas D. Sewell, Joel D. Kress, Edward M. Kober, Lily L. Wang, and Glenn Olah

LANSCE, T and MST Divisions, Los Alamos National Laboratory, Los Alamos, New Mexico 87545

Received: April 6, 2004; In Final Form: September 2, 2004

The vibrational spectra of three isotopomers of tetramethylammonium borohydride (TMAB) as well as of tetramethylammonium borofluoride were measured at 15 K by inelastic neutron scattering (INS). Direct analysis of the measured spectra was accomplished using classical molecular dynamics (MD) simulations and ab initio electronic structure theory for the crystalline solid. Comparison of observed and computed INS spectra revealed that the periodic electronic structure calculations for the crystalline solid provide a good description of the experimental INS spectrum and clearly demonstrates the power of this combined experimental/theoretical approach.

## I. Introduction

The intermolecular interactions of the tetramethylammonium (TMA) ion are of considerable importance in many areas of chemistry and biology for a variety of reasons, including its use as a structure-directing agent or template molecule in the synthesis of many nanoporous materials,<sup>1</sup> as a counterion for the crystallization of anionic metal clusters,<sup>2</sup> and its role in the understanding of the hydration of solutes with apolar surfaces in aqueous solutions. Despite the formally ionic character of TMA, the nature of its interactions with water, for example, are more of an apolar than ionic type.<sup>3</sup> An additional aspect of the interactions of TMA is the ability of the C–H groups to form relatively weak H-bonds with neighboring atoms such as O of the host material. In addition, the B–H bond has recently also been shown to be a fairly effective H-bond acceptor, so that the interaction between (TMA)<sup>+</sup> and (BH<sub>4</sub>)<sup>−</sup> could indeed give rise to what is now called a “dihydrogen bond”,<sup>4</sup> as proposed by Harmon and collaborators.<sup>5</sup>

A particularly effective way of studying the intermolecular interactions of TMA is the use of inelastic neutron scattering to obtain the vibrational spectra of the solid. This type of investigation has been carried out, for example, on many salts<sup>6</sup> of (TMA)<sup>+</sup> as well as TMA templates in a variety of zeolites.<sup>7</sup> These studies clearly demonstrate the great sensitivity of the low-frequency modes of this ion to the chemical environment.

Apart from the purely experimental spectroscopic indicators of the intermolecular interactions, complementary computational studies have become increasingly useful in that they provide a direct means for relating the experimental observations to the interatomic forces. Vibrational spectroscopy by INS is particularly useful in this regard since INS spectra can readily be calculated from the results (frequencies and atomic vibrational amplitudes) of both empirical or ab initio approaches, and hence a direct comparison of experimental and calculated vibrational spectra is possible.<sup>8</sup> This provides for an extremely powerful check of the interatomic interactions in the solid.

Tetramethylammonium borohydride (TMAB) is the simplest of the tetramethylammonium salts with boron-containing counterions. While the vibrational modes of the tetramethylammonium ion have been the subject of numerous studies,<sup>9–14</sup> little attention has been given in the literature<sup>5,15–17</sup> to TMAB, even though this system could be of use in understanding a wide range of order/disorder as well as structural phase transitions in many TMA salts, such as TMA tetrafluoroborate (see, for example, refs 18–20) and TMA perchlorate (see, for example, refs 21 and 22), and the question of the existence a novel H–H hydrogen bond<sup>4,5</sup> in TMAB.

In the present paper we focus on the vibrational spectroscopy of crystalline TMAB at 15 K. In particular, we use inelastic neutron scattering (INS) as an experimental probe of the vibrational modes of the molecular ions in the crystal. INS is very useful for this type of study since INS spectra contain information about all molecular and lattice modes as well as the interactions between them without any symmetry-based selection rules (see, for example, ref 23). Moreover, INS spectra can be readily computed from a knowledge of the frequencies and atomic displacements. This feature of INS is particularly amenable to existing theoretical methods. We therefore implemented ab initio electronic structure calculations with periodic boundary conditions as an aid in interpreting the experimental results. Such an approach has been used recently<sup>24</sup> to successfully model the vibrational modes in the INS spectra of crystalline tetramethylbenzene,<sup>24a</sup> benzoic acid,<sup>24b</sup> *N*-methylacetamide,<sup>24c</sup> RNA and DNA bases and nucleosides,<sup>24d</sup> and urea.<sup>24e</sup> The TMAB system is particularly interesting since it has a high density of hydrogenic atoms in two distinct chemical environments. By virtue of the large difference in neutron scattering cross-section for <sup>1</sup>H versus <sup>2</sup>H, selective deuteration of either the cation or the anion in TMAB allows for particularly incisive investigations into the vibrational and librational dynamics of the solid by INS.

The basic experimental and computational details are described in the following section. Results and discussion are

\* To whom correspondence should be addressed.

contained in sections III and IV, respectively. We conclude with final remarks and prospects for future studies in section V.

## II. Experimental Section

### a. Experimental Details.

Inelastic neutron scattering data were collected at  $T = 15$  K on the Filter Difference Spectrometer (FDS)<sup>25</sup> at the Manuel Lujan Jr. Neutron Scattering Center of Los Alamos National Laboratory. Spectra for normal TMAB, methyl deuterated, and boron-deuterated samples were obtained along with those for the  $(\text{BF}_4)^-$  salt as a reference for the TMA frequencies. Data were reduced by deconvolution of the instrumental function or maximum entropy methods.<sup>26</sup>

### b. Computational Details.

*Molecular Dynamics Calculations.* Molecular dynamics simulations of the crystal were performed using the InsightII/Discover suite of programs available from Molecular Simulations, Inc. (MSI), in conjunction with MSI's proprietary ESFF force field. The ESFF force field, which has been parametrized to accommodate all atoms through radon in the periodic table, is expressed in terms of covalent stretching, bending, and torsional interactions (diagonal terms only); 9–6 van der Waals nonbonded interactions; and atomic monopole–monopole electrostatic interactions. Details of the ESFF force field can be found in ref 27.

Although the space group and lattice parameters for TMAB have been reported,<sup>15</sup> a complete structure determination was not available at the time the present MD work was initiated. Thus, we generated a nominal initial crystal structure by combining the measured lattice parameters with the assumption that TMAB is isostructural with TMA tetrafluoroborate. The resulting unit cell was replicated into a  $2 \times 2 \times 2$  primary simulation cell, containing 352 atoms (256 H atoms), after which 40 ps of isothermal–isobaric (NpT) equilibration was performed at atmospheric pressure and a temperature of 15 K, with a step size of 1 fs. Long-range interactions were evaluated using Ewald sums. The Berendsen uniform dilation barostat was used throughout to maintain the measured shape of the crystal; simple velocity scaling and the Andersen thermostat were used to maintain the desired temperature during the first and second 20 ps segments, respectively. (These are standard options in the MSI software.) The average lattice parameters from the second 20 ps of NpT were used as input for isothermal–isochoric (NVT) equilibration. The protocol for the NVT equilibration was exactly analogous to that for the NpT segment. Finally, starting from the final phase space point of the NVT equilibration, a production run of length 20 480 fs was performed in the NVE ensemble using a step size of 0.25 fs. Configurations and velocities were saved to disk every 20 fs. The average temperature during the NVE run was 15 K.

Inelastic neutron scattering spectra were obtained within the one-phonon scattering approximation,<sup>23</sup> following the approach of Yip and co-workers<sup>28</sup>

$$\frac{d^2\sigma}{d\Omega d\omega} \propto \left[ \frac{E_f}{E_i} \right]^{1/2} \frac{q^2}{h\omega} f(\omega)$$

where  $h\omega$  is the transition energy;  $E_f = 3.6$  meV and  $E_i = E_f + h\omega$  are final and initial energies, respectively; and  $f(\omega)$  is the Fourier transform of the normalized velocity–velocity autocorrelation function for the protons

$$C_{vv}(\tau) = \frac{\langle v(\tau) \cdot v(0) \rangle}{\langle v(0) \cdot v(0) \rangle}$$

with ensemble averaging over all time origins and particle identities (as is appropriate to the present case of incoherent scattering). The relationship between  $q$  and  $h\omega$  is  $q = 0.695 \sqrt{2E_f + h\omega}$ , where  $q$  is in  $\text{\AA}^{-1}$  and  $h\omega$  is in meV. On the basis of the trajectory length and sampling interval, the spectral resolution and cutoff frequency of the calculated spectra are 1.6 and  $833 \text{ cm}^{-1}$ , respectively.

*Periodic Density Functional Theory Calculations.* The optimized structure for the unit cell of TMAB (containing two TMA and two borohydride ions) was calculated using the Vienna Ab Initio Simulation Package (VASP).<sup>29</sup> This code implements the Vanderbilt ultrasoft pseudopotential (USPP) scheme<sup>30,31</sup> to treat the valence electrons and the Perdew–Wang 91 parametrization<sup>32</sup> of the generalized gradient approximation (GGA) within the density functional theory for electronic structure. Three-dimensional periodic boundary conditions and a  $\Gamma$ -point sampling of the Brillouin zone were employed. The electronic wave functions are expanded in a plane wave basis set. The quality of the basis set is controlled by the planewave cutoff,  $E_{\text{cut}}$ . The setting  $\text{PREC} = \text{high}$  was used, which results in  $E_{\text{cut}} = 435$  eV = 1.25 times the recommended default value for the carbon atom USPP.

Vibrational frequencies and amplitudes were calculated using the finite difference scheme recently employed by Plazanet et al.<sup>24</sup> in a periodic DFT study of crystalline benzoic acid. Using the first derivatives of the energy in the form of Hellmann–Feynman forces for all atoms in the cell the Hessian matrix can be constructed. Each atom is displaced a distance  $\delta$  along each of the Cartesian directions (first in the positive, then in the negative direction) and a VASP energy calculation performed for each displacement. Central finite differences of the forces are then used to compute the second derivatives of the energy necessary to construct the full Hessian matrix. Vibrational modes and frequencies are obtained as the eigenvectors and eigenvalues, respectively, after diagonalizing the Hessian matrix. The frequencies calculated from the resulting force constant matrix are not scaled (in contrast to typical protocol for gas-phase calculations). The present implementation<sup>33</sup> was tested and compared by repeating the benzoic acid calculations of Plazanet et al.,<sup>24</sup> using their recommended Cartesian displacement value of  $\delta = 0.05 \text{ \AA}$ . For the largest frequencies (OH stretches), agreement to within 2% or better was found. For the smallest frequencies ( $< 100 \text{ cm}^{-1}$ ), the agreement was within 10% or better, which is acceptable considering the high sensitivity of the periodic DFT approach to low-frequency modes that depend heavily on weak intermolecular forces. Indeed, when the force constant calculation was performed with  $\delta = 0.01 \text{ \AA}$ , large frequencies ( $> 600 \text{ cm}^{-1}$ ) changed only negligibly while low frequencies ( $< 100 \text{ cm}^{-1}$ ) changed by factors of two or more. Choosing the right value for  $\delta$  for all vibrations is difficult in view of the wide range of frequencies and vibrational amplitudes to be analyzed.<sup>24a</sup> As discussed in ref 24c, the systematic variation of the calculated frequency with change in  $\delta$  may be ascribed to anharmonicity. In the case of methyl torsions, anharmonicity is expected to be large. In fact, methyl torsions have previously<sup>24a</sup> been treated explicitly as torsional oscillators. One additional complication was observed in the numerical calculation of the force constant matrix in Cartesian coordinates. In an exact calculation, three zero frequencies should be obtained for the translation and three positive frequencies for the libration of the center of mass. In practice, three zero frequencies are obtained for translation in all cases. However, for the librations, real and imaginary

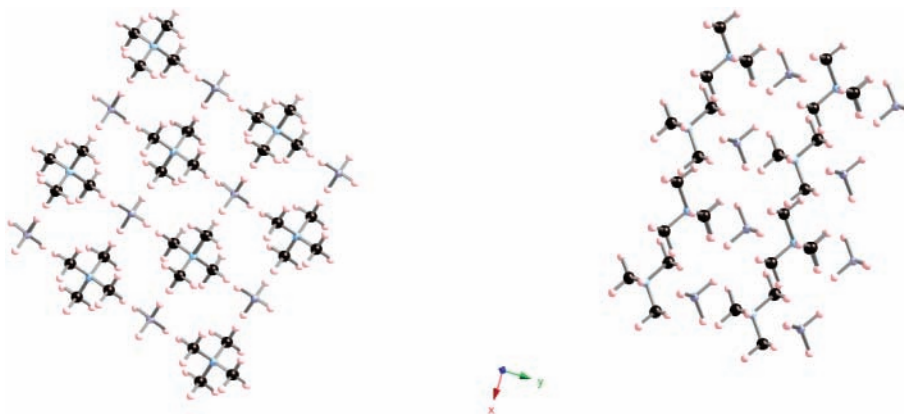


**Figure 1.** Tetramethylammoniumborohydride (TMAB) unit cell structure from computational studies:  $z$ - $y$  projection (left) and  $x$ - $y$  projection (right).

frequencies of small magnitude are found. For  $\delta = 0.01$  Å, the magnitude of the rotational frequencies is very small (of order of tens of  $\text{cm}^{-1}$ ). For  $\delta = 0.05$  Å, the value of one of the imaginary frequencies was  $100 \text{ cm}^{-1}$ . However, upon visualizing the normal modes of interest for comparison with the INS measurements, we concluded that the existence of the one imaginary frequency of  $100 \text{ cm}^{-1}$  does not indicate that calculation of the normal modes for frequencies of  $200 \text{ cm}^{-1}$  and greater is inaccurate. (We speculate that calculating the force constant matrix using finite differences based on approximate normal-mode coordinates would alleviate the problem of imaginary rotational frequencies. However, that approach is beyond the scope of the present work.) We therefore used a Cartesian displacement of  $\delta = 0.05$  Å in the results presented below. Frequencies and atomic vibrational amplitudes from the periodic DFT calculations were used to obtain a theoretical INS spectrum using the program CLIMAX<sup>34</sup> for direct comparison to experiment.

### III. Results

**Structure.** Structural parameters obtained in the MD calculations ( $T = 15$  K) and the periodic DFT calculations ( $T = 0$  K) compare favorably with the results from a recent single-crystal X-ray diffraction study at room temperature by Jackson et al.<sup>35</sup> when allowance is made for the difference in temperatures. Both the unit cell parameters and the positions of the atoms inside the cell were optimized in the theoretical studies. Unit cell parameters obtained are  $a = b = 7.7565$  Å,  $c = 5.549$  Å for symmetry-class-restricted MD and  $a = 7.723$  Å,  $b = 7.7762$  Å,  $c = 5.661$  Å for periodic DFT (ENCUT = 435 eV) compared with  $a = 7.8499$  Å,  $b = 7.8518$  Å,  $c = 5.60$  Å in the X-ray structure (space group  $P4/n$ ). The structure of the unit cell from the periodic DFT calculation is shown in Figure 1.

To check the sensitivity with respect to the planewave cutoff, a periodic DFT calculation with ENCUT = 566 eV was carried out, which yielded a net increase in the unit cell volume by 0.6% ( $a = 7.721$  Å,  $b = 7.764$  Å,  $c = 5.706$  Å).

The  $[\text{BH}_4]^-$  ion is orientationally disordered at room temperature, and the separation between the ion centers ( $\text{B}\cdots\text{N}$ ) is on average 4.74 Å. Intermolecular  $\text{C}-\text{H}\cdots\text{H}-\text{B}$  contact distances are in the range 2.32–2.59 Å (experiment) compared with 2.3–2.5 Å (MD) and 2.20 to 2.44 Å (DFT). The periodic DFT structure for the ion pair, however, resulted in a slightly closer approach of the two ions (i.e., an asymmetric structure was found with  $\text{B}\cdots\text{N}$  separations of 4.13 and 4.64 Å). In this configuration 3-fold axes of the TMA and  $[\text{BH}_4]^-$  ions are

parallel, and the relative orientations of the C–N and B–H bonds have a staggered arrangement. This close approach is likely to be the cause of the coupled low-frequency modes in the calculated spectra described below.

**Vibrational Spectra and Assignments.** The INS vibrational spectra of  $[(\text{CH}_3)_4\text{N}](\text{BH}_4)$ ,  $[(\text{CD}_3)_4\text{N}](\text{BH}_4)$ ,  $[(\text{CH}_3)_4\text{N}](\text{BD}_4)$ , and  $[(\text{CH}_3)_4\text{N}](\text{BF}_4)$  are shown in Figure 2a and b for frequency intervals of 100–2000 and 150–600  $\text{cm}^{-1}$ , respectively. It should be noted that deuteration of the methyl groups or the borohydride ion effectively “silences” the INS modes associated with the deuterated moiety so that, for example, the INS spectrum of  $[(\text{CD}_3)_4\text{N}](\text{BH}_4)$  shows principally the modes of the borohydride ion. Coupling among vibrational modes of the two ions could, however, give rise to some intensity for some modes of the deuterated ion. In addition, INS spectra have the property that all overtones and combinations (including those of internal lattice modes) are allowed and may have appreciable intensity.<sup>23</sup>

The internal vibrational modes of the TMA ion are normally treated as having an average point group symmetry of  $T_d$ , which results in the following 19 sets of normal modes

$$\Gamma = 3A_1 + 1A_2 + 4E + 4F_1 + 7F_2$$

which will be subject to factor group splittings in the solid as shown, for example, by Kabish.<sup>10</sup> Approximate descriptions of these normal modes and the observed INS frequencies below  $1500 \text{ cm}^{-1}$  are given in Table 1 along with those for the simple iodide salt<sup>6,10,12,13</sup> for reference purposes. There is no large variation in the internal mode frequencies of the TMA ion between those of the iodide salt and TMAB, and several of the factor group splittings are evidently resolved in the optical spectra but not in the INS measurements.

The  $(\text{BH}_4)^-$  ion is of tetrahedral symmetry and therefore has the usual four normal modes: two stretches and two deformations. In addition, we expect to observe at lower frequencies an intense INS band corresponding to the whole-body libration of the borohydride ion. The frequency observed for this mode in TMAB ( $207$ – $208 \text{ cm}^{-1}$ ) can be compared with those found by INS<sup>36</sup> for  $(\text{BH}_4)^-$  incorporated in alkali halide lattices, which range<sup>37</sup> from about 260 to  $360 \text{ cm}^{-1}$ . Librational frequencies in the latter are relatively high because of the H-bonding interactions with the alkali metal cations. We also suspect that this librational mode of  $(\text{BH}_4)^-$ , as well as some of the low-frequency vibrations of the TMA ion, will be coupled for this ion pair as is argued below. A comparison of the spectrum derived from the direct addition of the those of methyl- and



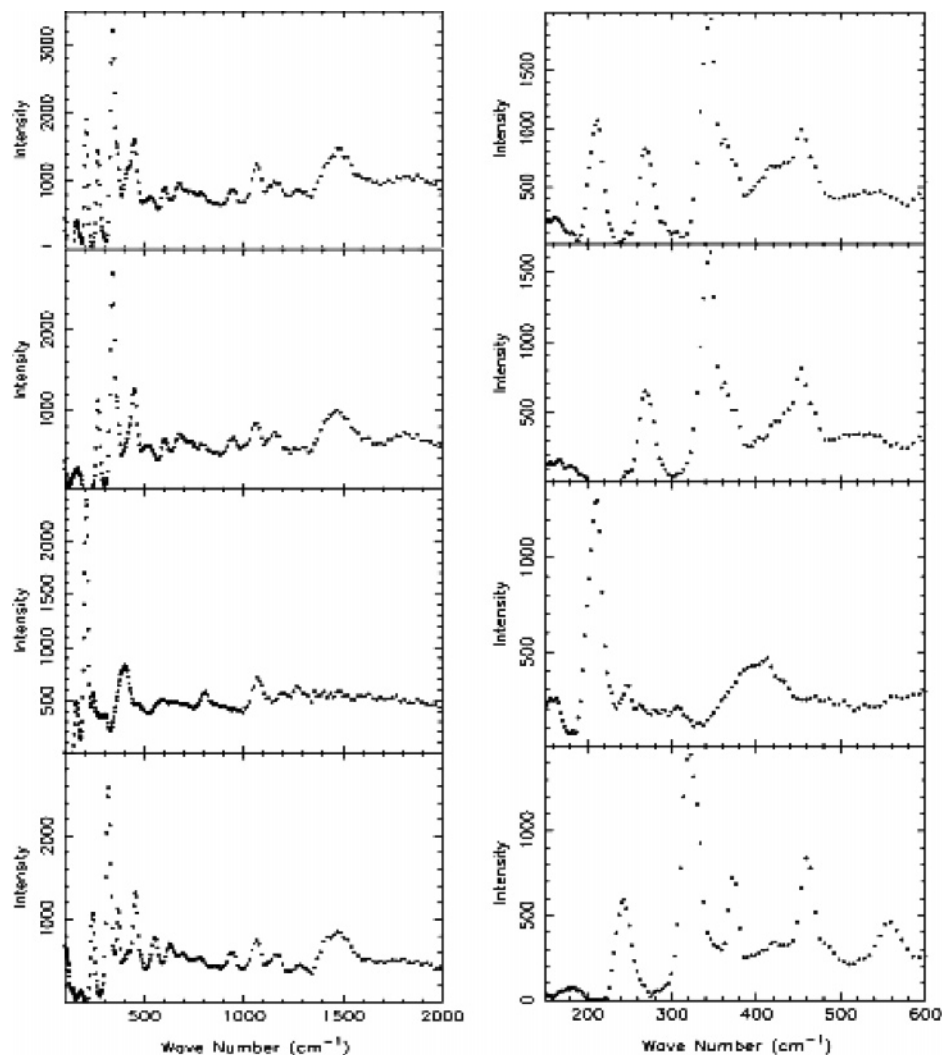


**Figure 2.** (a). Inelastic neutron scattering spectra (15 K) of (top to bottom) [TMA][BH<sub>4</sub>], [TMA][BD<sub>4</sub>], [TMA-d<sub>12</sub>][BH<sub>4</sub>], [TMA][BF<sub>4</sub>]. (b) Inelastic neutron scattering spectra (15 K) of (top to bottom) [TMA][BH<sub>4</sub>], [TMA][BD<sub>4</sub>], [TMA-d<sub>12</sub>][BH<sub>4</sub>], [TMA][BF<sub>4</sub>].

**TABLE 1: Observed INS Frequencies (cm<sup>-1</sup>) and Assignments for the TMA<sup>+</sup> and (BH<sub>4</sub>)<sup>-</sup> Ions**

TMA <sup>+</sup> Ion					
mode <sup>a</sup>	description	TMA[BF <sub>4</sub> ]	TMA[BD <sub>4</sub> ]	TMA[BH <sub>4</sub> ]	[TMA]I <sup>a</sup>
$\nu_4$	torsion	238	265	265	265 <sup>a</sup>
$\nu_{12}$	torsion	316	337	337	344 <sup>a</sup>
$\nu_8$	C <sub>4</sub> N def.	366	366	366	367/380
$\nu_{19}$	C <sub>4</sub> N def.	451	445	446	451 <sup>a</sup>
$\nu_3$	C <sub>4</sub> N sym str.	766	788	779	749/754
$\nu_{18}$	C <sub>4</sub> N asym str.	948	943	944	943
$\nu_7$	CH <sub>3</sub> rock (E)	1163	1167	1152	1174/1181
$\nu_{11}$	CH <sub>3</sub> rock (F <sub>1</sub> )	1070	1062	1057	1074
$\nu_{17}$	CH <sub>3</sub> rock (F <sub>2</sub> )	1287	1276	1280	1284

(BH <sub>4</sub> ) <sup>-</sup> Ion			
mode <sup>b</sup>	description	TMA[BH <sub>4</sub> ]	[(CD <sub>3</sub> )N][BH <sub>4</sub> ]
	[BH <sub>4</sub> ] <sup>-</sup> torsion	208	207
$\nu_4$	[BH <sub>4</sub> ] <sup>-</sup> deformation	<i>b</i>	1070
$\nu_2$	[BH <sub>4</sub> ] <sup>-</sup> deformation	<i>b</i>	1200/1280

<sup>a</sup> References 2, 4, 5, and 28. <sup>b</sup> These modes overlap with modes of the TMA ion and could not be separately assigned.

B-deuterated TMAB with that of fully protonated TMAB does indeed reveal some noticeable discrepancies in the intensities of the TMA torsional bands ( $\nu_4$  and  $\nu_{12}$ ) and of (BH<sub>4</sub>)<sup>-</sup> which would not be expected if these modes were completely uncoupled.

## IV. Discussion

**Hydrogen Bonding.** The possible existence of hydrogen bonding between the methyl and borohydride hydrogens in TMAB was first proposed by Harmon et al.<sup>5</sup> on the basis of observed shifts in the C–H stretching region. The presence of such hydrogen bonds has only recently been conclusively established.<sup>4</sup> Our INS spectra are inconclusive as to the existence of such an interaction: while the torsional bands  $\nu_4$  and  $\nu_{12}$  of TMA are shifted to significantly higher frequency in the presence of the (BH<sub>4</sub>)<sup>-</sup> ion when compared with the (BF<sub>4</sub>)<sup>-</sup> ion pair, these modes have even higher frequencies in the TMA halides for which hydrogen bonding is known to be significant. Large variations in the torsional modes (for example, 206 to 245 cm<sup>-1</sup> for  $\nu_4$ ) also occur for TMA template ions in various zeolites,<sup>7</sup> which may also represent varying degrees of hydrogen bonding between C–H and framework oxygen atoms. Both the experimental<sup>35</sup> and our theoretical structural results support the conclusion that the H···H hydrogen bonding may be less important in TMAB as all such intermolecular contacts here are found to be greater than 2.3 Å (i.e., close to or greater than the sum of the van der Waals radii of 2.4 Å).

**Comparison between Experiment and Theory.** The experimental INS spectrum of normal TMAB is compared in Figure 3 to the results of the molecular dynamics (MD) simulation and the DFT calculation. Both the MD simulations

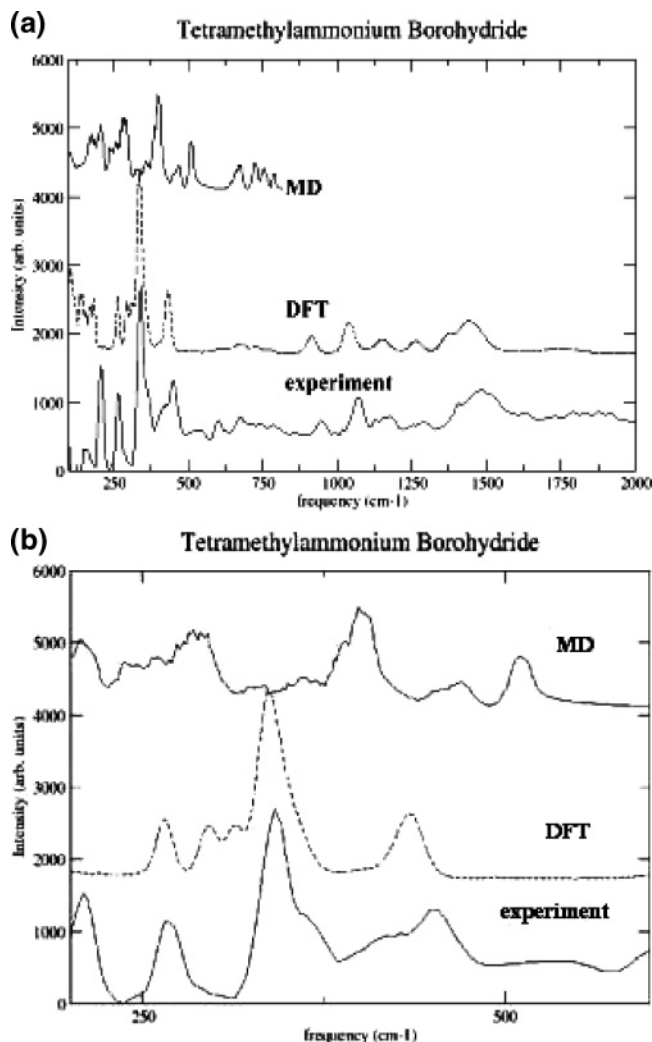


**Figure 3.** Measured (experiment) and calculated INS spectra for TMAB are shown for two frequency ranges: (a) 100–2000 and (b) 200–600  $\text{cm}^{-1}$ . The MD and DFT calculations are for the periodic crystalline solid. Each spectrum is scaled independently such that the most intense peak has unit intensity.

and DFT calculations utilize periodic boundary conditions and should account for intermolecular effects provided the intermolecular forces are suitably described with classical force fields and DFT model chemistry, respectively.

The low-frequency modes found in these calculations are generally coupled translational or librational modes of the ion pair. These would give rise to optical phonons or librations for the solid. Descriptions of these modes in the following discussion are based on visualization of the eigenvectors obtained from the periodic DFT calculations. The strongest peak in the INS spectrum, the methyl torsion  $\nu_{12}$  at 337  $\text{cm}^{-1}$ , is overestimated by the force field used for the MD simulation, where the methyl torsion appears at approximately 400  $\text{cm}^{-1}$ . The periodic DFT calculations reproduce the experimental data remarkably well (see Table 2), both in terms of relative intensities and frequencies, between 350 and 750  $\text{cm}^{-1}$ . The periodic DFT methyl torsion peaks, at 270 and 330  $\text{cm}^{-1}$ , and the C–N deformation bands, at 360 (shoulder) and 440  $\text{cm}^{-1}$ , agree quite well with the position of the peaks in the INS spectra. The libration of the  $[\text{BH}_4]^-$  ion is observed in the INS at 208  $\text{cm}^{-1}$ . The MD simulation shows a broad band in this region. The periodic DFT calculations show two bands for the  $[\text{BH}_4]^-$  libration at around 185 and 228  $\text{cm}^{-1}$ , centered about the INS peak.

**TABLE 2: Observed INS Frequencies vs Periodic DFT Calculations for TMA $[\text{BH}_4]$**

obsd frequency ( $\text{cm}^{-1}$ )	calcd frequency ( $\text{cm}^{-1}$ )
208	185 228 <sup>a</sup>
265	270
337	330
366	360
446	438
779	735

<sup>a</sup> Asymmetry in structure leads to splitting into two peaks. See text.

The librational frequency of the  $[\text{BH}_4]^-$  ion in a series of alkali halides has been empirically observed<sup>36</sup> to depend on the mean cation–anion separation ( $a_0$ ) as  $a_0^{-3}$ . If we use the value<sup>36</sup> of 262  $\text{cm}^{-1}$  for  $[\text{BH}_4]^-$  in KI (where  $a_0 = 3.533 \text{ \AA}$ ) one would expect the librational frequency for  $[\text{BH}_4]^-$  in TMAB ( $a_0 = 4.74 \text{ \AA}$ ) to occur at approximately 108  $\text{cm}^{-1}$  instead of the observed value of 208  $\text{cm}^{-1}$ . If such a comparison is even approximately valid, one can conclude that a substantial portion of the intramolecular interactions between the ion pair  $[\text{TMA}]^+$  and  $[\text{BH}_4]^-$  may include some level of C–H $\cdots$ H–B dihydrogen bonding in addition to nonbonded interactions.

## V. Summary

The present comparative study between experiment, molecular dynamics simulations, and periodic ab initio calculations of the INS vibrational spectra of TMAB clearly demonstrates the power of this combined experimental/theoretical approach. The periodic DFT electronic structure calculations predict frequencies that agree well with the INS measured frequencies over the entire spectral range considered and result in a calculated INS vibrational spectrum that gives an excellent account of the experimental observation. Some remaining discrepancies in the low-frequency region between 150 and 500  $\text{cm}^{-1}$  may well be attributed to anharmonicities in the librational modes. The generic ESFF force field employed in the MD studies, on the other hand, yields less reliable predictions.

**Acknowledgment.** The authors thank Prof. J. E. Jackson and collaborators for communicating the results of their X-ray diffraction study of TMAB and Dr. B. Uberuaga for providing the periodic DFT Hessian calculation program. This work was supported by the United States Department of Energy under contract number W-7405-ENG-36 with the University of California. The work has benefited from the use of facilities at the Manuel Lujan Jr., Neutron Scattering Center, a National User Facility funded as such by the United States Department of Energy, Office of Science.

## References and Notes

- (1) Suib, S. L. *Chem. Rev.* **1993**, 93, 803.
- (2) See, for example: Bau, R.; Drabnis, M. H.; Gralschelli, L.; Klooster, W. T.; Xie, Z.; Koetzle, T. F.; Martinego, S. *Science* **1997**, 75, 1099.
- (3) Turner, J. Z.; Soper, A. K.; Finney, J. L. *J. Chem. Phys.* **1995**, 102, 5438.
- (4) Crabtree, R. H.; per Siegbahn, P. E. M.; Eisenstein, O.; Rheingold, A. L.; Koetzle, T. F. *Acc. Chem. Res.* **1996**, 29, 348.
- (5) Harmon, K. M.; Gennici, I.; Madeira, S. L. *J. Phys. Chem.* **1974**, 78, 2585.
- (6) Ratcliffe, C. I.; Waddington, T. C. *J. Chem. Soc., Faraday Trans. 2* **1976**, 72, 1935.
- (7) Newsam, J. M.; Brun, T. O.; Trouw, F. R.; Iton, L. E.; Curtiss, L. A. In *Novel Materials in Heterogeneous Catalysis*; Baker, R. T. K., Murrell, L. L., Eds.; ACS Symposium Series 437; American Chemical Society: Washington, D.C., 1990; p 25.
- (8) Condensed Phase Structure and Dynamics: a Combined Neutron Scattering and Numerical Modelling Approach. Special issue of *Chemical*

*Physics*, Johnson, M. R., Kearley, G. J., Eckert, J., Eds.; Elsevier: Amsterdam, The Netherlands, 2000, Vol. 261, pp 1–274.

- (9) Wilson, W. W.; Christe, K. O. *Inorg. Chem.* **1989**, *28*, 4172.
- (10) Kabish, G. *J. Raman Spectrosc.* **1980**, *9*, 279.
- (11) Berg, R. W. *Spectrochim. Acta* **1978**, *34A*, 655.
- (12) Krishnamurthy, N. *Proc. Ind. Acad. Sci.* **1965**, *61*, 164.
- (13) Bottger, G. L.; Geddes, A. L. *Spectrochim. Acta* **1965**, *21*, 1701.
- (14) Young, C. W.; Koehler, J. S.; McKinney, D. S. *J. Am. Chem. Soc.* **1947**, *69*, 1410.
- (15) King, A. J.; Kanda, F. A.; Russell, V. A.; Katz, W. *J. Am. Chem. Soc.* **1956**, *78*, 4176.
- (16) Semenenko, K. N.; Kravchenko, O. V.; Shilkin, S. P. *Z. Neorg. Khim.* **1975**, *20*, 2334.
- (17) Guillevic, G.; Maillot, F.; Mongeot, H.; Dazord, J.; Cueilleron, J. *Bull. Soc. Chim. Fr., I: Physicochim. Syst. Liq. Electrochim. Catal. Gen. Chim.* **1977**, 1977, 1099.
- (18) Giuseppetti, G.; Mazzi, F.; Tadini, C.; Ferloni, P.; Torre, S. *Z. Kristallogr.* **1992**, *202*, 81.
- (19) Torre, S.; Ferloni, P. *Z. Naturforsch.* **1992**, *47a*, 721.
- (20) Palacios, E.; Melero, J. J.; Burriel, R.; Ferloni, P. *Phys. Rev. B* **1996**, *54*, 9099.
- (21) McCullough, J. D. *Acta Crystallogr.* **1964**, *17*, 1067.
- (22) Ilyukhin, A. B.; Malyarik, M. A. *Cryst. Rep.* **1995**, *40*, 704.
- (23) Eckert, J. *Spectrochim. Acta A* **1992**, *48*, 271. Boutin, H.; Yip, S. *Molecular Spectroscopy With Neutrons*; Boutin, H., Yip, S., Eds.; MIT Press: Cambridge, 1968.
- (24) (a) Plazanet, M.; Johnson, M. R.; Gale, J. D.; Yilirim, T.; Kearley, G. J.; Fernandez-Diaz, M. T.; Sanchez-Portal, D.; Artacho, E.; Soler, J. M.; Ordejon, P.; Garcia, A.; Trommsdorff, H. P. *Chem. Phys.* **2000**, *265*,

189. (b) Plazanet, M.; Fukushima, N.; Johnson, M. R.; Horsewill, A. J.; Trommsdorff, H. P. *J. Chem. Phys.* **2001**, *115*, 3241. (c) Kearley, G. J.; Johnson, M. R.; Plazanet, M.; Suard, E. *J. Chem. Phys.* **2001**, *115*, 2614. (d) Plazanet, M.; Fukushima, N.; Johnson, M. R. *Chem. Phys.* **2002**, *280*, 53. (e) Johnson, M. R.; Parlinski, K.; Natkaniec, I.; Hudson, B. S. *Chem. Phys.* **2003**, *291*, 53.

(25) Taylor, A. D.; Wood, E. J.; Goldstone, J. A.; Eckert, J. *Nucl. Instrum. Methods Phys. Res.* **1984**, *221*, 408.

(26) Sivia, D. S.; Vorderwisch, P.; Silver, R. N. *Nucl. Instr. Methods A* **1990**, *290*, 492.

(27) *Discover User Guide*, Oct 1995; Biosym/MSI: San Diego, California, 1995; pp 3-19–3-28.

(28) Anderson, J.; Ullo, J. J.; Yip, S. *J. Chem. Phys.* **1987**, *86*, 4078.

(29) Kresse, G.; Hafner, J. *Phys. Rev. B* **1993**, *47*, RC558. Kresse, G.; Furthmuller, J. *Comput. Mater. Sci.* **1996**, *6*, 15. Kresse, G.; Furthmuller, J. *Phys. Rev. B* **1996**, *54*, 11169.

(30) Vanderbilt, D. *Phys. Rev. B* **1990**, *41*, 7892.

(31) Kresse, G.; Hafner, J. *J. Phys. Condens. Matter* **1994**, *6*, 8245.

(32) Wang, Y.; Perdew, J. P. *Phys. Rev. B* **1991**, *44*, 13298. Perdew, J. P.; Chevary, J. A.; Vosko, S. H.; Jackson, K. A.; Pederson, M. R.; Singh, D. J.; Fiolhais, C. *Phys. Rev. B* **1992**, *46*, 6671.

(33) Uberuaga, B.; Stumpf, R.; Windl, W. Unpublished work.

(34) Kearley, G. J. *J. Chem. Soc., Faraday Trans. 2* **1986**, *82*, 41. Kearley, G. J. *Nucl. Instrum. Methods A* **1995**, *354*, 53.

(35) Jackson, J. E. Personal communication.

(36) Brierley, K. P.; Howard, J.; Waddington, T. C. *J. Chem. Soc., Faraday Trans. 2* **1981**, *77*, 1075.

(37) Smith, D. *Can. J. Chem.* **1988**, *66*, 791.